Polymer 50 (2009) 4182–4188

Contents lists available at ScienceDirect

Polymer

journal homepage: www.elsevier.com/locate/polymer

Impact of thickness on CO_2 concentration profiles within polymer films swollen near the critical pressure

Xinxin Li, Bryan D. Vogt*

Department of Chemical Engineering, Arizona State University, Tempe, AZ 85284, USA

ARTICLE INFO

Article history:
Received 10 April 2009
Received in revised form
22 June 2009
Accepted 28 June 2009
Available online 3 July 2009

Keywords:
Supercritical fluids
Carbon dioxide
Interfaces

ABSTRACT

The isothermal swelling of polymer thin films by a supercritical fluid does not increase monotonically with increasing chemical potential (pressure), but rather a maximum in swelling is generally observed near the critical pressure. A reactive templating approach utilizing the condensation of silica within hydrophilic domains of a swollen amphiphilic polymer film enables visualization of the qualitative concentration profile of CO_2 by the changes in the size of hydrophobic domains (pores) with cross sectional TEM microscopy; specifically, isothermal swelling of poly(ethylene oxide-propylene oxide-ethylene oxide) films by CO_2 at 60 °C is examined. Films that contain thickness gradients are used to avoid any uncertainties in the impact of thickness due to variations in the temperature or pressure during the silica modification. A uniform pore size (local swelling) is observed for all film thicknesses when the pressure is outside of the anomalous maximum in the film swelling, except for a small increase at the buried interface due to preferential adsorption of CO_2 to the native silicon oxide surface of the substrate. However at this swelling maximum, a gradient in the pore size is observed at both interfaces. These swelling gradients at interfaces appear to be responsible for the anomalous maximum in thin films. As the film thickness increases beyond 350 nm, there is a decrease in the maximum swelling at the free interface.

1. Introduction

Supercritical carbon dioxide has been proposed as alternative green solvent for the processing of polymeric materials due to being environmentally benign with tunable solvent quality through manipulation of the fluid density through temperature and/or pressure [1,2]. However, most polymers are not soluble in CO_2 [3], but generally can be appreciably swollen [4]. The sorption of CO_2 into polymers leads to changes in their physical properties including a decrease in the glass transition temperature (T_g) [5], an increase in the diffusivity of the polymer chains [6], and changes in the phase behavior of multicomponent polymeric systems [7–9]. The improvements in the transport properties of CO_2 swollen polymers enable improvements in processing of some otherwise intractable materials [10].

The potential for significant improvements in physical properties exists through the incorporation of nanofillers to create polymer nanocomposites. These nanocomposites have been proposed for use in a host of applications ranging from lightweight structural materials to membranes for separations [11,12]. Their processing can be difficult due to the presence of the filler materials, especially when the nanomaterial is highly asymmetric such as in the case of carbon nanotubes. CO_2 has been recently explored as a green alternative for aiding in the processing of polymer nanocomposites [13]. However, it is still unclear how CO_2 interacts within these nanocomposites. One report for PMMA–clay nanocomposites showed that swelling can be solely attributed to the PMMA and is consistent with neat PMMA [14]; but the changes in viscosity of polymer-fumed silica nanocomposites swollen with CO_2 is dependent upon the surface chemistry of the nanofillers [15]. Thus, an improved fundamental understanding of the physical interactions between CO_2 and polymer nanocomposites would be useful. Recently, several groups have reported on the equivalence of polymer thin films and nanocomposites in regards to the thermophysical properties [16,17]. Therefore, thin films provide an attractive surrogate to probe the fundamental properties of polymer nanocomposites as both films and nanocomposites exhibit large surface area to volume ratios. Understanding interfaces in thin films can provide insight into the behavior of analogous polymer nanocomposites. Additionally, CO_2 processing of polymeric thin films has been shown to be advantageous for some photoresist systems [18] and in the fabrication of low-*k* dielectric films [19] for microelectronics. In these applications, precise control

* Corresponding author. Tel.: +1 480 727 8631.
E-mail address: bryan.vogt@asu.edu (B.D. Vogt).

0032-3861/$ – see front matter © 2009 Elsevier Ltd. All rights reserved.
doi:10.1016/j.polymer.2009.06.069

of the structure is required at the nanoscale. Thus, it is important to understand where CO_2 goes in these thin films, especially in regards to the polymer interfaces.

These interfaces are thermodynamically distinct from the bulk of the polymer and provide a different potential for absorbing species. Supported polymer thin films can exhibit apparent changes in the solubility of solvents. In particular, water in polymer thin films has been examined extensively using neutron reflectivity [20,21] and to a lesser degree using ion scattering [22]. An accumulation (or depletion) of water at the polymer–substrate interface measured with reflectivity can be directly correlated to changes in the apparent solubility with decreasing film thickness [23]. A qualitatively similar phenomenon has been observed for the swelling of polymer thin films with carbon dioxide [24,25]. However, film swelling in this case is not monotonic; an anomalous maximum in the swelling is observed at a CO_2 activity near unity [24–26]. Unlike water, the distribution of CO_2 within the films is difficult to quantify directly as the neutron contrast between most polymers and CO_2 is low.

Recently, we reported an indirect route to visualize the CO_2 concentration profiles using an *in-situ* reactive templating approach [27]. This is based upon the seminal work of Watkins and co-workers that demonstrated that reactions with CO_2 swollen polymers [28,29] can be used fabricate well defined nanoporous structures using amphiphilic templates [19]. After allowing an amphiphilic film to equilibrate with CO_2, the local swelling of the hydrophobic domains can be determined by the selective *in-situ* condensation of silica within the hydrophilic domains, which "locks" the swollen size into the templated structure. This process enabled the identification of long range gradients in the CO_2 concentration in polymer films swollen near the density fluctuation ridge [30] (near critical point). A gradient extending approximately 150 nm into the film from the free surface and a short ($<$10 nm) gradient at the buried interface is found for a 350 nm thick film prepared at CO_2 pressure corresponding to the anomalous swelling maximum [27].

However, the CO_2 swelling of polymer thin films appears to be dependent upon initial thickness [25,31]. For example, Koga et al. found that absolute swelling amount decreases as increasing film thickness at anomalous swelling and levels off when initial thickness h_0 approaches $8R_g$ (polymer radius of gyration) for deuterated polybutadiene (d-PB) polymer thin films [32]. In this work, the impact of film thickness on CO_2 concentration gradients is examined using the previously described *in-situ* reactive templating approach. To avoid difficulties in obtaining identical processing conditions, thickness gradient films produced using flow coating [33] are utilized to assess multiple thicknesses simultaneously. These results provide insight into CO_2 sorption at free and buried (polymer/native silicon oxide) interfaces near the anomalous swelling maximum.

2. Experimental section

2.1. Materials and synthesis

Polymer templates were prepared from solutions containing poly(ethylene oxide)-*b*-poly(propylene oxide)-*b*-poly(ethylene oxide) (Pluronic F108, BASF), poly(*p*-hydroxystyrene) (PHOSt, $M_n = 8000$ g/mol, DuPont Electronic Materials), and *p*-toluenesulfonic acid (*p*-TSA, Aldrich) dissolved in a mixture of ethanol (Aldrich) and deionized water. The use of a hydrogen bonding polymer blend yields a highly ordered template that is not possible from the Pluronic alone [34–36]. This extended ordering simplifies the identification of any gradients in the film after reaction. Silicon wafers were utilized as substrates and were cleaned using UV/Ozone cleaner (Jelight Company Inc. Model 42) for a cleaning time of 5 min prior to film formation. A schematic of the flow coating [33] technique used to create a gradient polymer template film is illustrated in Fig. 1(a). The apparatus consists of a glass blade fixed above a movable stage. A bead of the polymer solution is deposited between the glass blade and substrate and then the stage is accelerated. The variation in frictional drag with respect to blade velocity determines the amount of the polymer solution left behind. A constant acceleration rate during the flow coating results in a film with a near linear gradient in thickness (Fig. 1b) until the blade decelerates.

The gradient polymer films are then placed in a closed stainless steel vessel (25 mL, Thar) preheated to 60 °C and pressurized slowly with CO_2 to desired pressure. The polymer film was then allowed to equilibrate with the CO_2. Reactive modification of the CO_2 swollen polymer template used a fixed quantity of precursors (10 μL of tetraethyl orthosilicate (TEOS, Aldrich) and 20 μL deionized water) for all syntheses. All the reactions were allowed to proceed for 30 min, then the reactor was slowly de-pressurized to avoid foaming of the resultant silica–polymer nanocomposite. To increase the robustness of the films for visualization, a post-synthesis aging in a sealed vessel with saturated water vapor at 90 °C for 2 h was used to enhance silica network formation followed by calcination at 450 °C for 5 h at a heating rate of 1 °C/min in air to remove the organic template.

2.2. Film characterization

Spectroscopic ellipsometry (SE) and transmission electron microscopy (TEM) were utilized to characterize the film

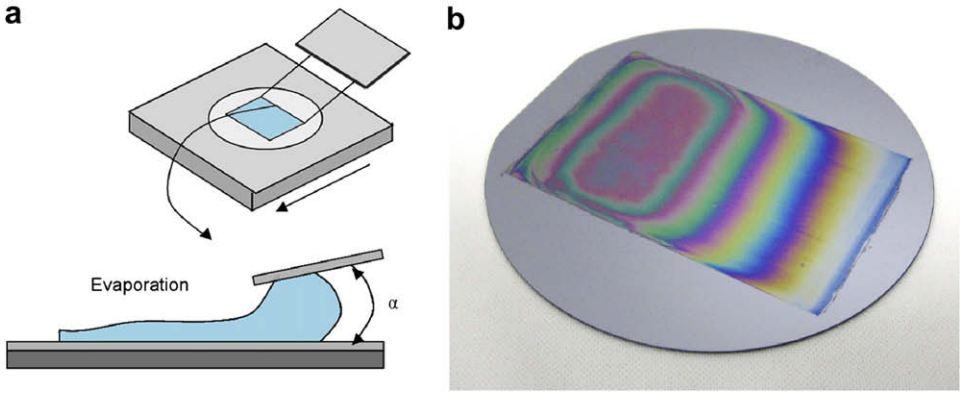

Fig. 1. (a) Schematic of the flow coating process, where α is the glass blade angle to the substrate. The substrate is moving in the direction of the arrow. (b) A gradient film coated by flow coater. Color variance indicates thickness difference.

morphology. Ellipsometry was used to characterize the evolution of the film thickness and refractive index in processing with a UV–visible–NIR (240–1700 nm) Variable Angle Spectroscopic Ellipsometer (VASE M-2000, J.A. Woollam Co.). The Cauchy model effectively approximates the optical properties of the polymeric template, the silica–polymer nanocomposite after reaction and the mesoporous silica film. The thickness gradient was mapped using SE with step size of 1.5 mm along the direction of gradient change using WVASE Manager (J.A. Woollam Co.). The Bruggemann Effective Medium Approximation (BEMA) model was used to calculate the film porosity (P) based upon the film refractive index by assuming the mesoporous film consists of silica framework with a fixed refractive index [37] and voids. TEM micrographs were obtained using JEOL 2010F operating at 200 keV. TEM cross sections were prepared by manual polishing of a cut section of the film/substrate at different positions along the thickness gradient films.

The pore size distribution (PSD) of the film was determined using ellipsometric porosimetry (EP) utilizing toluene (Aldrich) as the probe solvent. Mass flow controllers (MKS) are used to mix controlled fractions of saturated toluene vapor in air and neat air streams to vary the relative partial pressure of toluene ($0 < P/P_0 < 1$). Both adsorption and desorption isotherms were measured. The EP data were analyzed on the basis of the change in refractive index as a function of relative pressure [38] and the PSD was calculated by application of the Kelvin equation.

3. Results and discussion

Processing through silica reaction and calcination to remove the polymeric template creates changes in the thickness of the films as quantified using SE (Fig. 2). Originally, these films vary nearly linearly in thickness from approximately 1400 nm down to 200 nm; this graded thickness varies gradually over 80 mm across the coating. Prior studies examining the anomalous swelling maximum in polymer thin films have shown potential thickness effects in this range [25,31]. After the TEOS condensation reaction, the film thickness increases by approximately 50% compared to its original thickness when the film is preswollen at 70 bar, but this thickness change decreases to ≈15% when swollen at 87 bar (near anomalous maximum in swelling as reported previously [27]). This change in thickness is related to variations in the reaction extent within the film as a function of CO_2 pressure. The partitioning of small molecules between polymer and CO_2 phases is highly sensitive near fluid phase activities of unity [39], which leads to an anomalous maximum in the swelling behavior of polymer films near this chemical potential. Thus, we hypothesize that the differences in thickness between the two conditions are due to a decrease in concentration of TEOS within the polymer film at 87 bar in comparison to 70 bar. Due to the differences in the silica incorporation between these two conditions, comparison of total porosity of the films will not provide any information regarding pore size gradients that would be indicative of CO_2 concentration gradients.

During calcination, the films contract due to the polymer template removal and additional condensation of residual silanol groups in the silica network. For the gradient films prepared at 87 bar, this contraction is greater in the thinner region, up to 80% decrease in thickness from the post-reaction film in the thinnest sections. In contrast, the film processed outside of the anomalous maximum region contracts less for the thinnest film region (≈30% contraction in thickness during calcination from that after TEOS condensation reaction). From the refractive indices of the film, the porosity can be determined using EMA model [40] as shown in Fig. 2c and d. The film synthesized near the anomalous swelling maximum at 87 bar yields a near constant porosity, which is approximately 70%, in the thickest regions, but the porosity increases when the porous film (after calcination) thickness is decreased to less than 400 nm. A maximum in porosity (approximately 85%) is observed around a thickness of 200 nm. As the film thickness further decreases, porosity then decreases down to approximately 50% for a film that is nearly 30 nm thick. One reason for the lower porosity for the very thin film below 100 nm is the partial collapse of the film due to large film contraction in this region as discussed previously. In Fig. 2d, the porosity of the gradient film prepared at 70 bar is nearly constant through the full thickness range at approximately 30%, but there is an increase in

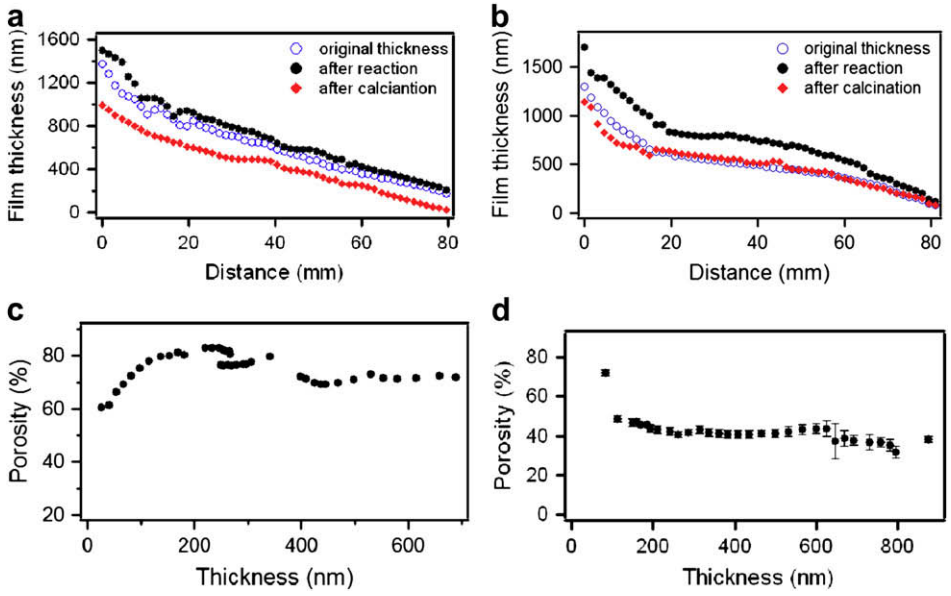

Fig. 2. Thickness of gradient film (○) as cast, (●) after reaction with TEOS, and (◆) after calcination for films prepared at CO_2 pressure of (a) 87 bar and (b) 70 bar. The porosity of the films is calculated from the refractive indices. The porosity as a function of the porous film thickness is illustrated for synthesis at CO_2 pressure of (c) 87 bar and (d) 70 bar. The porosity is a convolution of reaction extent, pore size, and film contraction from calcination.

porosity for thicknesses less than 200 nm. This is consistent with the decreased contraction for the thin sections of the film synthesized at 70 bar. These differences in the contraction through the film thickness and porosity suggests that there is a morphological difference that is dependent upon the pressure at which the polymer is swollen, but this cannot be de-convoluted from differences in the reaction extent.

A better measure of the swelling of the hydrophobic domains prior to condensation of the silica network can be obtained through the pore size distribution (PSD). To obtain PSD, ellipsometric porosimetry utilizing toluene capillary condensation within the pores was employed across the gradient at fixed spacings. Adsorption and desorption isotherms as shown in Fig. 3 were obtained by monitoring changes in the refractive index of the film upon exposure to varying partial pressures of toluene as described in previous studies [40]. By examining gradient thickness films prepared at both 70 bar and 87 bar, the influence of film thickness on the average pore size and its distribution in the mesoporous silica films is elucidated as shown in Fig. 3. For the film exposed to CO_2 at 70 bar prior to silica condensation, the average pore size is invariant with thickness. This is expected as CO_2 swelling of thin polymer films at this pressure do not exhibit the anomalous behavior and thus the film is expected to be swollen uniformly. The width of the pore size distribution is quite narrow, consistent with a templated process; however the width does increase for the thinnest film (115 nm) thickness examined. This is a relatively minor change in the PSD, but does suggest that there might be a small excess of CO_2 at one of the interfaces, even away from the anomalous maximum. From the previous work, an increase in pore size (CO_2 concentration) near the silicon substrate interface might be occurring at this pressure, but it was not statistically significant [27]. Conversely, the PSD for the mesoporous films prepared in the vicinity of CO_2 critical pressure at 87 bar exhibits a strong thickness dependence as illustrated in Fig. 3b. The PSD significantly broadens as the thickness is decreased. This result is consistent with a long range CO_2 concentration gradient within the polymer film prior to

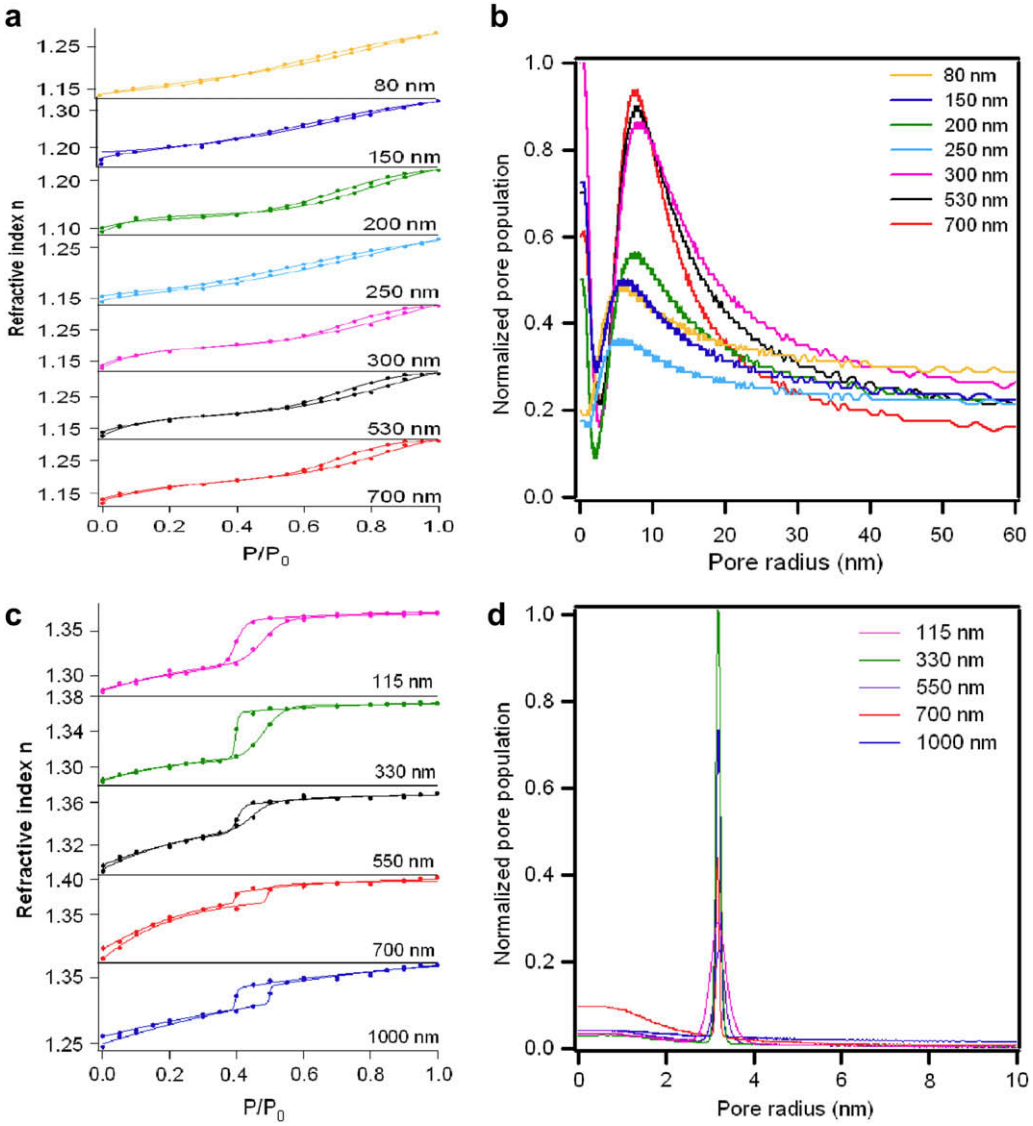

Fig. 3. Adsorption and desorption isotherms for toluene in mesoporous silica films prepared at (a) 87 bar and (c) 70 bar. Measurements were performed on thickness gradient films. Isotherms were determined by the changes in the refractive index ($\lambda = 632$ nm) of the silica film as a function of the adsorbate (toluene) relative pressure. Calculated pore size distribution based upon the desorption branch of the isotherms at (b) 87 bar and (d) 70 bar. For the film synthesized at a CO_2 pressure of 87 bar, PSDs are broader compared to the film at 70 bar.

reaction with TEOS. However, there appears to be a major break in the PSD at a film thickness of approximately 300 nm. Thinner films exhibit a very broad PSD, while thicker films are much narrower. This suggests that the CO_2 concentration gradient might be thickness dependent with a decrease in the extent of the variation in the concentration profile when the film thickness exceeds approximately 300 nm.

Prior work from Koga et al. demonstrated that the anomalous swelling of polybutadiene increases for films thinner than approximately $8R_g$ [32]; this is consistent with the changes in the PSD shown here if the anomalous swelling results from gradients in the CO_2 concentration within the film. As the film thickness increases, the gradient fraction in the film appears to decrease as the PSD narrows and the fractional swelling also is reported to decrease [32]. Similarly, Green and co-workers examined the film thickness dependence of the anomalous swelling in thin films for several different polymers and generally found a decrease in the swelling at the maximum as the thickness increased [31]. However, examination of the data shows that the swelling cannot be modeled as two constant interfacial swollen layers and a bulk-like middle of the film that is dependent upon the film thickness [31]. This result suggests that the gradients in CO_2 concentration through the film are dependent upon the finite film thickness, or there are additional factors that increase the swelling of the films relative to the bulk. One explanation for the anomalous swelling that does not invoke swelling gradients within the polymer is critical wetting where adsorption of dense CO_2 at the surface occurs [41]. The presence of a swelling gradient within the polymer film does not preclude an adsorbed layer as well. For the reactive templating used in this work, an adsorbed layer of CO_2 on the polymer surface would not impact the film structure and only the CO_2 concentration within the film can be probed. However if the gradient at the film surface is invariant, this would suggest that there is indeed an adsorbed layer as this would explain the difficulties in modeling the film thickness dependence [31].

To determine the size of the gradients within the porous films, cross sections of the films are visualized using transmission electron microscopy. As shown in Figs. 4 and 5, the porous films exhibit a cubic microstructure, which is consistent with previous work using Pluronic F108 as a template [40]. For the film synthesized at 70 bar shown in Fig. 4, the pore radius appears to be uniform through the thickness of the film for both 100 nm and 600 nm sections. Conversely for the films prepared at 87 bar shown in Fig. 5, the pore size appears to be significantly larger at the free surface and silicon substrate interfaces than in the center of the film, especially for the cross sections of the thinner sections. The inset in Fig. 5a better illustrates the different pore sizes for a small section of the film with two equal length black bars for reference. Near the free interface (bottom bar), the pores are larger than the bar as part of the pore is still visible when overlaid. Conversely near the middle of the film, the bar is the same dimension as a pore. For the thickest section (approximately 700 nm), the pores appear to be nearly uniform in size. This is consistent with a thickness dependent CO_2 gradient near the anomalous swelling maximum and could explain difficulties with simple explanations in describing the CO_2 swelling of polymer films with varying thickness at the anomalous maximum [31].

These micrographs reveal significant differences in the pore size dependent upon film thickness and CO_2 pressure to which the film was exposed. The changes in the pore radius parallel to the film surface provide indirect evidence for the size of the CO_2 concentration profiles that were present within the swollen polymer films. Previous work has demonstrated that for CO_2 pressures less than the anomalous maximum that the pore size change in reference to a film exposed to the vapor pressure of TEOS (no CO_2) is quantitatively consistent with bulk swelling of the same hydrophobic polymer [28]. Thus by measuring the pore radius as a function of distance from the silicon substrate, the approximate local concentration of CO_2 within the film can be determined; however this is only quantitative at pressures near or greater than the anomalous maximum pressure as will be discussed later. As shown in Fig. 6, the average pore size (as determined from multiple micrographs of different areas in each cross section) for the two different thicknesses of the mesoporous film prepared at 70 bar is statistically invariant through the film thickness irrespective of film thickness except very close ($<$10 nm) to the silicon substrate. CO_2 is known to form an adsorbed layer on silica surfaces [42], thus an accumulation of CO_2 at this buried interface is not surprising (the silicon wafer has native oxide (silica) at its surface). However since the condensation of TEOS forms a silica–polymer interface *in-situ* at the pore wall during the reaction, the pores might be swollen to a greater extent than expected for bulk swelling. This leads to uncertainty in the correspondence of pore size and local CO_2 concentration and thus these micrographs only provide a qualitative measure of the CO_2 concentration profiles. For the film exposed to 87 bar of CO_2, there is a large gradient in the pore size at the film/air surface where the pore radius is approximately 6.5 nm for thicknesses of 200 nm and 350 nm, but decreases steadily over nearly 150 nm into the film to approximately 3.8 nm for the thicker film. Additionally, there is a sharp increase in the pore size close to the silicon substrate. This increased pore size at the buried interface is significantly larger

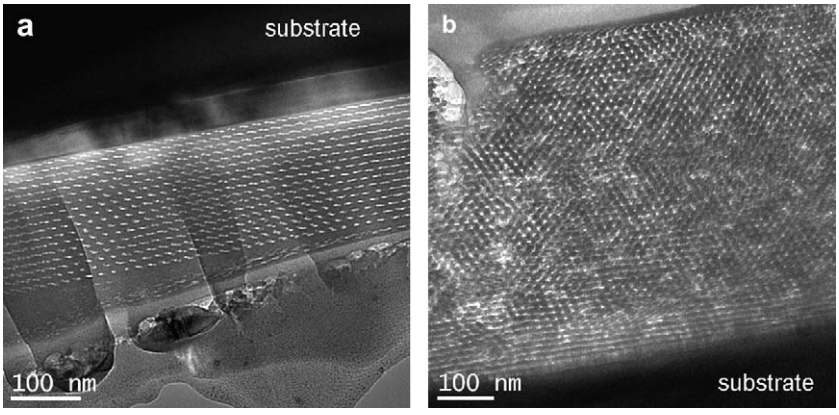

Fig. 4. Transmission electron micrographs of calcined mesoporous silica films synthesized using CO_2 at 70 bar. Images were taken at a thickness of (a) 180 nm and (b) 600 nm.

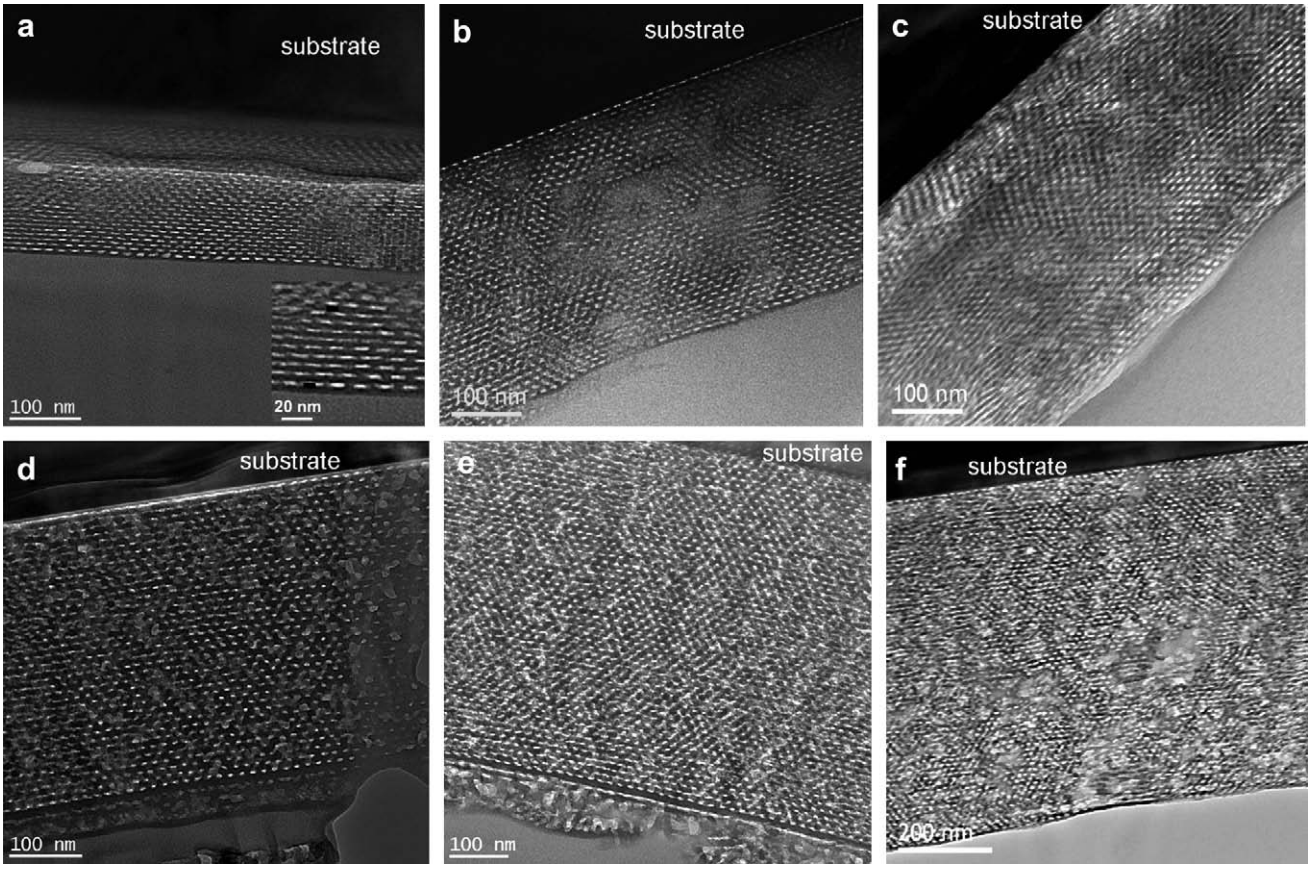

Fig. 5. Transmission electron micrographs of calcined mesoporous silica films synthesized using CO_2 at 87 bar. For thickness below 350 nm, images (a) and (b), the pore size gradient can be determined by visual inspection. To improve the clarity of these pore size differences, an inset for the near surface of the thinnest film is included in (a) with two equal length bars included. Note that the bar in the middle of the film extends completely across the in-plane thickness of the pores, while near the free surface the pores are larger than the bar. For thickness around 400 nm (c), the pore size gradient becomes smaller. For even thicker film (d) 420 nm, (e) 600 nm, and (f) 700 nm, the pore size gradient is not clearly evident to the naked eye.

than observed at the lower pressure (70 bar). However when the thickness of the film is increased to greater than 400 nm, a more uniform pore size is observed, which is consistent with the breadth of the PSD obtained from EP. An intermediate behavior is observed for the 400 nm thick section where the extent of pore size gradient at the free interface is smaller than observed for thinner sections. For even thicker films, 600 nm and 700 nm film, the pore size gradient is further decreased at the free interface. Interestingly, there is also a decrease in the pore size at the buried interface as the thickness is increased as well. These results suggest that the anomalous swelling of polymer films by CO_2 is a result of concentration gradients, but the size and extent of these gradients are dependent upon the polymer film thickness.

The length scale of the perturbation in the apparent CO_2 concentration at the buried interface is minor in comparison to the gradient at the free surface when the integrated effect on the film swelling is considered [27]. However, the adsorption of CO_2 at the buried silicon substrate strongly influences the adsorption of CO_2 at the film/air free interfaces. This would suggest a coupling of the properties of the free surface of the film to the substrate over quite long length scales. However, Torkelson and co-workers have demonstrated using fluorescence labeling that the surface T_g of polystyrene films is strongly dependent upon the chemical nature of the supporting interface [43]. This coupling between the substrate and the free surface can effect the local surface T_g even when the film is hundreds of nm thick. The reported thickness dependent CO_2 concentration gradients at the free surface are

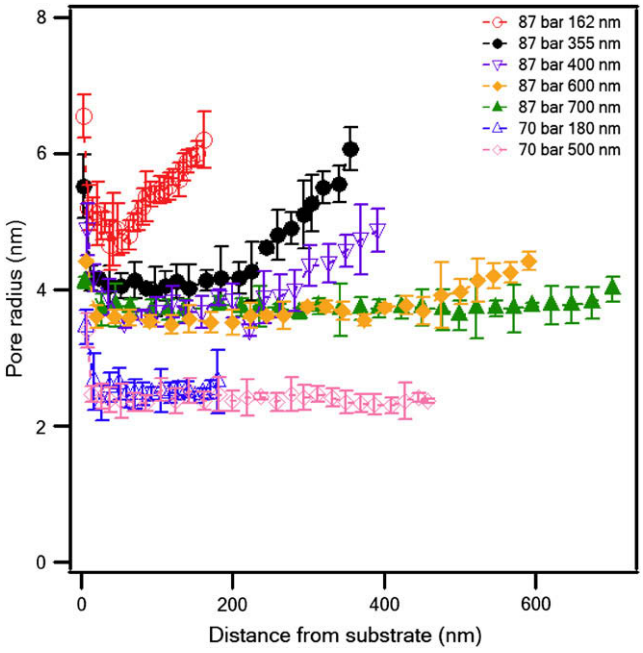

Fig. 6. Dependence of pore size on location within the gradient films for (△) 180 nm, (◇) 500 nm thick films synthesized at a CO_2 pressure of 70 bar, and at 87 bar for (○)162 nm, (●)355 nm, (▽) 400 nm, (◆) 600 nm and (▲) 700 nm thick films. The pore size is determined from TEM micrograph cross sections.

consistent with the impact of substrate chemistry on the surface T_g. One issue that arises is the disagreement with theory based upon the Sanchez–Lacombe equation of state (SLEOS) coupled with gradient theory, which suggests the adsorption of a dense layer of CO_2 to the polymer film surface (critical wetting) is the source of the anomalous swelling [41]. Generally, SLEOS provides at least a qualitative description of polymer physics, but it should be noted that the reactive templating approach utilized here will not provide any information about a critical wetting layer. However, near the critical point for ternary phase metal alloys, relatively large compositional gradients occur at the interfaces between phases through adsorption of a minority component [44]. By analogy, the critical wetting of a dense CO_2 layer at the surface of the polymer film near the critical point of CO_2 also provides a three phase system with adsorption of a minority phase (critical wetting layer) at the interface between the other two phases. Thus, we hypothesize that the gradients at the polymer free surface might result from compositional dependencies on the free energy near the critical point as a result of a CO_2 adsorption layer. The thickness dependence of the gradient would then be dependent upon the critical wetting layer, which would be a function of the intermolecular and surface force [45]. Thus, variation in the polymer film thickness would alter the Hamaker coefficient, and hence the adsorbed CO_2 layer on the polymer film. Simulations and additional theoretical work are necessary to provide further physical insight into the nature of the anomalous swelling of polymer films by fluids near their critical point.

4. Conclusions

The local swelling of amphiphilic films by CO_2 was indirectly determined using a selective reactive modification methodology to generate a porous film that enables visualization of standing concentration gradients within the films. TEM cross section micrographs identified gradient in pore size extending into the film from the free surface and a short ($<$10 nm) gradient at the buried interface near the pressure where the anomalous maximum in swelling is observed for polymer thin films. However, these gradients in pore size that are related to the local CO_2 concentration are strongly dependent upon the thickness of the film. The extent of the gradient in size difference at both interfaces decreases as the film becomes thicker. Conversely, a uniform pore size through the film thickness is observed at lower pressure except for a small increase at the buried interface. These results suggest a coupling between the substrate and free surface over length scales of 100's of nanometer through the polymer film, potentially due to critical wetting.

Acknowledgements

The authors acknowledge support from the National Science Foundation under Grant No. CBET-0746664. We thank DuPont Electronic Materials (Jim Sounik and Michael Sheehan) for donation of the poly(4-hydroxystyrene). BDV thanks Monica Olvera de la Cruz for helpful discussion regarding gradients near critical conditions for ternary systems. We acknowledge the use of facilities in the LeRoy Erying Center for Solid State Science in Arizona State University.

References

[1] Tomasko DL, Li HB, Liu DH, Han XM, Wingert MJ, Lee LJ, et al. Ind Eng Chem Res 2003;42:6431–56.
[2] Woods HM, Silva MMCG, Nouvel C, Shakesheff KM, Howdle SM. J Mater Chem 2004;14:1663–78.
[3] Sarbu T, Styranec T, Beckman EJ. Nature 2000;405:165–8.
[4] Sato Y, Yurugi M, Fujiwara K, Takishima S, Masuoka H. Fluid Phase Equilib 1996;125:129–38.
[5] Wissinger RG, Paulaitis ME. J Polym Sci Part B Polym Phys 1991;29:631–3.
[6] Gupta RR, Lavery KA, Francis TJ, Webster JRP, Smith GS, Russell TP, et al. Macromolecules 2003;36:346–52.
[7] Vogt BD, RamachandraRao VS, Gupta RR, Lavery KA, Francis TJ, Russell TP, et al. Macromolecules 2003;36:4029–36.
[8] Walker TA, Colina CM, Gubbins KE, Spontak RJ. Macromolecules 2004;37:2588–95.
[9] Watkins JJ, Brown GD, RamachandraRao VS, Pollard MA, Russell TP. Macromolecules 1999;32:7737–40.
[10] Garcia-Leiner M, Lesser AJ. J Appl Polym Sci 2004;93:1501–11.
[11] Merkel TC, Freeman BD, Spontak RJ, He Z, Pinnau I, Meakin P, et al. Science 2002;296:519–22.
[12] Shiflett MB, Foley HC. Science 1999;285:1902–5.
[13] Tomasko DL, Han XM, Liu DH, Gao WH. Curr Opin Solid State Mater Sci 2003;7:407–12.
[14] Manninen AR, Naguib HE, Nawaby AV, Day M. Polym Eng Sci 2005;45:904–14.
[15] Flichy NMB, Lawrence CJ, Kazarian SG. Ind Eng Chem Res 2003;42:6310–9.
[16] Bansal A, Yang HC, Li CZ, Cho KW, Benicewicz BC, Kumar SK, et al. Nat Mater 2005;4:693–8.
[17] Rittigstein P, Priestley RD, Broadbelt LJ, Torkelson JM. Nat Mater 2007;6:278–82.
[18] Felix NM, Tsuchiya K, Ober CK. Adv Mater 2006;18:442.
[19] Pai RA, Humayun R, Schulberg MT, Sengupta A, Sun JN, Watkins JJ. Science 2004;303:507–10.
[20] Kent MS, Smith GS, Baker SM, Nyitray A, Browning J, Moore G. J Mater Sci 1996;31:927–37.
[21] Wu WL, Orts WJ, Majkrzak CJ, Hunston DL. Polym Eng Sci 1995;35:1000–4.
[22] Wallace WE, Chiou TT, Rothman JB, Composto RJ. Nucl Instrum Meth B 1995;103:435–9.
[23] Vogt BD, Soles CL, Jones RL, Wang C-Y, Lin EK, Wu W, et al. Langmuir 2004;20:5285–90.
[24] Koga T, Seo YS, Zhang YM, Shin K, Kusano K, Nishikawa K, et al. Phys Rev Lett 2002;89:125506.
[25] Sirard SM, Ziegler KJ, Sanchez IC, Green PF, Johnston KP. Macromolecules 2002;35:1928–35.
[26] Koga T, Akashige E, Reinstein A, Bronner A, Seo YS, Shin K, et al. Physica B Condensed Matter 2005;357:73–9.
[27] Li X, Vogt BD. Macromolecules 2008;41:9306–11.
[28] Watkins JJ, Mccarthy TJ. Macromolecules 1994;27:4845–7.
[29] Watkins JJ, Mccarthy TJ. Chem Mater 1995;7:1991–4.
[30] Nishikawa K, Tanaka I, Amemiya Y. J Phys Chem 1996;100:418–21.
[31] Li Y, Park EJ, Lim KTL, Johnston KP, Green PF. J Polym Sci Part B Polym Phys 2007;45:1313–24.
[32] Koga T, Seo YS, Shin K, Zhang Y, Rafailovich MH, Sokolov JC, et al. Macromolecules 2003;36:5236–43.
[33] Stafford CM, Roskov KE, Epps TH, Fasolka MJ. Rev Sci Instrum 2006;77.
[34] Tirumala VR, Daga V, Bosse AW, Romang A, Ilavsky J, Lin EK, et al. Macromolecules 2008;41:7978–85.
[35] Tirumala VR, Pai RA, Agaarwal S, Testa JJ, Bhatnagar G, Romany AH, et al. Chem Mater 2007;19:5868–74.
[36] Tirumala VR, Romang AH, Agarwal S, Lin EK, Watkins JJ. Adv Mater 2008;20:1603–8.
[37] Palik ED. Handbook of optical constants, vol. 1. Orlando: Academic Press; 1985. p. 579.
[38] Baklanov MR, Mogilnikov KP, Polovinkin VG, Dultsev FN. J Vac Sci Technol B 2000;18:1385–91.
[39] Kazarian SG, Brantley NH, West BL, Vincent MF, Eckert CA. Appl Spectrosc 1997;51:491–4.
[40] Li X, Vogt BD. Chem Mater 2008;20:3229–38.
[41] Wang XC, Sanchez IC. Langmuir 2006;22:9251–3.
[42] Sirard SM, Castellanos H, Green PF, Johnston KP. J Supercrit Fluids 2004;32:265–73.
[43] Roth CB, McNerny KL, Jager WF, Torkelson JM. Macromolecules 2007;40:2568–74.
[44] Huang C, De la Cruz MO, Voorhees PW. Acta Materialia 1999;47:4449–59.
[45] Israelachvili J. Intermolecular and surface forces. London: Academic Press; 1992.